Pancreatology xxx (xxxx) xxx

Contents lists available at ScienceDirect

Pancreatology

journal homepage: www.elsevier.com/locate/pan

Determining age and sex-specific distribution of pancreatic whole-gland CT attenuation using artificial intelligence aided image segmentation: Associations with body composition and pancreatic cancer risk

Laurens P. Janssens [a], Alexander D. Weston [b], Dhruv Singh [c], Grant Spears [d], William S. Harmsen [d], Naoki Takahashi [e], Kenneth A. Philbrick [e], Bradley J. Erickson [e], Barham K. Abu Dayyeh [c], Suresh T. Chari [c], Vinay Chandrasekhara [c], Ferga C. Gleeson [c], Michael J. Levy [c], Randall K. Pearson [c], Bret T. Petersen [c], Santhi Swaroop Vege [c], Shounak Majumder [c, *]

[a] Department of Internal Medicine, Mayo Clinic, Rochester, MN, USA
[b] Department of Biomedical Statistics and Informatics, Mayo Clinic, Jacksonville, FL, USA
[c] Department of Gastroenterology and Hepatology, Mayo Clinic, Rochester, MN, USA
[d] Department of Biomedical Statistics and Informatics, Mayo Clinic, Rochester, MN, USA
[e] Department of Radiology, Mayo Clinic, Rochester, MN, USA

ARTICLE INFO

Article history:
Received 21 February 2021
Received in revised form
24 July 2021
Accepted 17 August 2021
Available online xxx

Keywords:
Pancreatic steatosis
Pancreatic ductal carcinomas
Artificial intelligence
Deep learning
Convolutional neural network

ABSTRACT

Background & aims: Increased intrapancreatic fat is associated with pancreatic diseases; however, there are no established objective diagnostic criteria for fatty pancreas. On non-contrast computed tomography (CT), adipose tissue shows negative Hounsfield Unit (HU) attenuations (−150 to −30 HU). Using whole organ segmentation on non-contrast CT, we aimed to describe whole gland pancreatic attenuation and establish 5th and 10th percentile thresholds across a spectrum of age and sex. Subsequently, we aimed to evaluate the association between low pancreatic HU and risk of pancreatic ductal adenocarcinoma (PDAC).

Methods: The whole pancreas was segmented in 19,456 images from 469 non-contrast CT scans. A convolutional neural network was trained to assist pancreas segmentation. Mean pancreatic HU, volume, and body composition metrics were calculated. The lower 5th and 10th percentile for mean pancreatic HU were identified, examining the association with age and sex. Pre-diagnostic CT scans from patients who later developed PDAC were compared to cancer-free controls.

Results: Less than 5th percentile mean pancreatic HU was significantly associated with increase in BMI (OR 1.07; 1.03−1.11), visceral fat (OR 1.37; 1.15−1.64), total abdominal fat (OR 1.12; 1.03−1.22), and diabetes mellitus type 1 (OR 6.76; 1.68−27.28). Compared to controls, pre-diagnostic scans in PDAC cases had lower mean whole gland pancreatic HU (−0.2 vs 7.8, p = 0.026).

Conclusion: In this study, we report age and sex-specific distribution of pancreatic whole-gland CT attenuation. Compared to controls, mean whole gland pancreatic HU is significantly lower in the pre-diagnostic phase of PDAC.

1. Introduction

Visceral fat excess has several well-known deleterious effects on health and metabolism. The impact of excess fat accumulation in the pancreas remains poorly understood. The lack of objective thresholds for diagnosis of excess intrapancreatic fat on abdominal

* Corresponding author. Department of Gastroenterology and Hepatology, Mayo Clinic, 200 First street SW, Rochester, MN, 55905, USA.
E-mail address: Majumder.Shounak@mayo.edu (S. Majumder).

https://doi.org/10.1016/j.pan.2021.08.004
1424-3903/

imaging, the non-uniform distribution of intrapancreatic fat, and the inherent risks associated with obtaining pancreatic tissue for a histologic diagnosis are major barriers to an informed interpretation of the clinical implications of excess intrapancreatic fat. Several different terms have been used in the medical literature to describe excess intrapancreatic fat further highlighting the general lack of consensus. Fatty pancreas (FP), which is the term we will use in this study, and pancreatic steatosis are the most commonly used terms used to describe excess fat accumulation in the pancreas [1–3].

The association between obesity and increased risk of pancreatic ductal adenocarcinoma (PDAC) is well established [4–6]. Small case-control studies have reported increased intrapancreatic fat in the tumor-free regions of resected PDAC specimens compared to healthy controls [7,8]. However, it is unclear whether this increase in intrapancreatic fat represents a primary process driving carcinogenesis or is secondary to parenchymal atrophy due to tumor-associated ductal obstruction. Data from animal models suggest that intrapancreatic fatty infiltration and obesity-driven adipokines, cytokines and other pro-inflammatory factors can activate oncogenic *KRAS* signaling, resulting in an increased risk of pancreatic intraepithelial neoplasia and progression to pancreatic cancer [9].

Currently, there are no widely accepted objective diagnostic criteria for FP [10]. Pancreatic biopsy is an invasive procedure associated with risk of bleeding and pancreatitis, and thus generally avoided unless targeting a solid or cystic lesion concerning for neoplasia. Hence noninvasive imaging is the favored modality for clinical diagnosis of FP. However, radiological studies have shown that the distribution of intrapancreatic fat is heterogeneous, leading to a significant risk of sampling error if using regions of interest (ROIs) [11]. Different radiological modalities have been studied to assess intrapancreatic fat. A hyperechoic pancreas on ultrasonography is often labeled as FP, although ultrasonography results are highly operator-dependent and influenced by the patient's body habitus [12–14]. Proton magnetic resonance spectroscopy (1H-MRS) has been proposed as a modality for assessing intrapancreatic fat. However, its use remains largely limited to research studies because of technical challenges in clinical application [15,16]. A relatively newer technique, 3D Iterative Decomposition with Echo Asymmetry and Least Squares Estimation (IDEAL)-MRI, has faster image acquisition and less signal contamination, rendering it an appealing technique for fat quantification of small organs such as the pancreas [17,18]. Nevertheless, magnetic resonance imaging (MRI) is expensive and results still need validation in large healthy cohorts to define accurate diagnostic cutoffs for fatty pancreas across a spectrum of age and sex. Furthermore, most studies to date have used ROIs to measure pancreas fat content rather than whole gland quantification, again raising the possibility of sampling error [16–20]. This was confirmed in a recent study by Kato et al., who performed MRI-based whole-pancreas fat analysis on a cohort of 159 patients with nonalcoholic fatty liver disease. They found that there was significant variability in fat fraction between smaller ROIs in the same region of the pancreas (i.e., head, body, or tail), reflecting the patchy and heterogeneous pattern of intrapancreatic fat [21]. The lack of reliable and objective criteria for diagnosing fatty pancreas has been a limiting factor in the further study of associations between intrapancreatic fat and risk of pancreatic cancer.

On non-contrast computed tomography (CT), adipose tissue shows negative Hounsfield Unit attenuations (−150 to −30 HU) [22]. However, setting an intensity threshold of −30 to −150 is unlikely to be accurate for measuring intrapancreatic fat, which is a mix of fat and pancreatic tissue, due to partial volume effects [23]. Since the distribution of intrapancreatic fat is heterogeneous, measurement of mean whole pancreas attenuation would allow for a more accurate non-invasive surrogate estimate of total intrapancreatic fat. However, there are no prior studies that have measured whole-gland pancreas attenuation in a healthy population and hence the normal distribution remains unknown. The primary objective of our study was to measure whole gland pancreatic Hounsfield Unit (HU) on non-contrast abdominal CT scans in a cohort of adults without known underlying pancreatic disease and establish the 5th and 10th percentile thresholds for mean pancreatic HU across a spectrum of age and sex. We subsequently aimed to study the association of mean pancreatic HU with body composition and metabolic parameters and compare the mean pancreatic HU in pre-diagnostic abdominal CT scans in PDAC patients with cancer-free controls.

2. Materials and methods

We identified all non-contrast CT abdomen examinations at our institution between 1/1/2015 and 1/1/2016. A total of 9,784 CT abdomen examinations were identified. All clinical radiology reports were documented by expert-radiologists indicating the presence of pancreatic disease or prior pancreatic surgery and excluded from the study if either was present. Reports describing excess pancreatic fat (i.e. 'fatty pancreas', 'fatty infiltration of the pancreas', 'fatty replacement of the pancreas', 'fatty atrophy of the pancreas', and 'pancreatic steatosis') without other pancreatic disease were not excluded. The remaining 8,543 examinations were divided into 12 different groups based on sex (male or female) and age category (18–30 years old; 31–40 years old; 41–50 years old; 51–60 years old; 61–70 years old; >70 years old). From each group, 60 examinations were randomly selected for analysis. Of the resulting 720 examinations, 251 had to be excluded due to unavailability of appropriate non-contrast images, incomplete visualization of the pancreas, or the presence of image artifacts (such as metal artifacts from implanted devices).

In the remaining 469 examinations, the entire pancreas was segmented using the medical imaging dataset annotation software tool RIL-Contour [24]. Initial annotations were manually performed by L.J. To expedite the annotation process, after manual segmentation of a sufficient number of CT examinations had been performed (295 full organ segmentations total), a deep convolutional neural network (CNN) based on the U-Net architecture was trained on this subset of the data. The U-net was transfer-learned from a prior segmentation model [25]. In all cases, segmentations performed with the deep-learning model were reviewed and manually corrected when necessary. From these segmentation masks, mean and median pancreatic HU were calculated as the mean and median values of all pixels contained in the segmentation mask. Pancreatic volume (cm^3) was also calculated as the sum of the number of pixels in the segmentation mask multiplied by pixel dimensions, which were derived from the DICOM image header. These calculations were performed using Python 2.7.10 (Python Software Foundation, Beaverton, OR). Additionally, 3D volumes of abdominal subcutaneous fat, visceral fat, and skeletal muscle in a 10 cm range centered on the L3 vertebra (cm^3) were calculated using a separate, previously-developed CNN [26]. Demographic characteristics including body mass index (BMI), history of diabetes mellitus and hemoglobin A1c level were retrieved from the electronic health record.

Categorical variables were analyzed using Fisher's exact test. Continuous variables were analyzed using the nonparametric Kruskal-Wallis test. The correlation between mean and median pancreatic HU was assessed with the Spearman method. The 5th and 10th percentiles of mean pancreatic HU were calculated, conditional on age and sex, using quantile regression [27]. Based on the significant age and sex associations that were found (considering

p < 0.05 as significant), appropriate one-sided 5% or 10% reference ranges were estimated and considered as potential diagnostic indicators of fatty pancreas. Associations between these indicators and abdominal fat distribution, muscle mass, BMI, and glycemic status were tested by means of logistic regression analysis. Statistical analysis was performed using SAS 9.4 (SAS Institute).

Next, using electronic medical record data repository software (Advanced Cohort Explorer), we identified patients at our institution diagnosed with PDAC on whom non-contrast CT imaging of the pancreas was available at a date before but within two years of eventual radiological diagnosis of PDAC. These pre-diagnostic scans were reviewed to exclude presence of a visible pancreatic mass. Mean pancreatic HU and pancreatic volume (cm^3) were calculated on these pre-diagnostic CT scans using methods described above. These cases were compared in a 1:2 ratio to age (±2 years), sex, and diabetes mellitus matched controls without PDAC. All controls were manually screened to ensure no diagnosis of PDAC was made in the 5 years after index CT scan. Univariate and multivariate logistic regression analysis was done to detect differences between mean pancreatic HU, pancreatic volume and BMI between cases and controls. This study was approved by the Mayo Clinic Institutional Review Board (IRB#16–007866 and 18–010737).

3. Results

Fig. 1 demonstrates pancreas segmentation in RIL-Contour on axial slices with real time reconstruction of the coronal and sagittal views. Table 1 shows the demographic data and summarizes examination parameters in the study population categorized by sex. Mean pancreatic HU and median pancreatic HU were highly correlated using Spearman's test for correlation (r = 0.98869; p = <0.0001) and thus only mean pancreatic HU was reported in the results. There was no significant difference in mean BMI between females and males (30.7 vs 29.6; p = 0.1242). Mean pancreatic volume was significantly higher in males compared to females (97.53 cm^3 vs 74.76 cm^3; p = <0.0001). Mean pancreatic HU was significantly lower in males compared to females (11.4 vs 19.4; p = <0.0001).

There was no difference in pancreatic volume between individuals with and without diabetes mellitus. However, mean pancreatic HU was significantly lower in patients with diabetes mellitus compared to those without (1.1 vs 19.6; p = <0.0001) [Supplementary Table 1]. Additionally, pancreatic examination parameters and body metrics were evaluated per BMI category. Pancreatic volume increased with increasing BMI whereas mean pancreatic HU decreased with increasing BMI. Subcutaneous fat, visceral fat, total fat, and muscle volumes all significantly increased with increasing BMI [Supplementary Table 2].

Spearman rank correlation test between mean pancreatic HU on the one hand and age, BMI, pancreatic volume, and body metrics on the other hand was calculated [Supplementary Table 3]. Mean pancreatic HU decreased with increasing age, BMI, subcutaneous fat volume, visceral fat volume and muscle volume. No significant correlation between mean pancreatic HU and pancreatic volume was found.

Using quantile regression, a significant sex association was found for mean pancreatic HU at both the 5th percentile (p = 0.027) and 10th percentile (p = 0.002). After stratifying by sex, age was also significantly associated with these percentiles, linearly for the 5th and 10th percentile in males and 5th percentile in females, and in quadratic form for the 10th percentile in females. Overall, at these lower quartiles, mean pancreatic HU decreased with age in both sexes (Fig. 2). The specific 5th and 10th percentile thresholds of mean pancreatic HU per age and sex category were calculated (data not shown) [Supplementary Table 4].

In our study a total of 26 subjects had a mean pancreatic HU below 5th percentile and 23 were between 5th-10th percentiles. All CT scans for subjects below the 10th percentile cutoff were reviewed by an expert pancreatic radiologist (N.T.) who was blinded to the mean pancreatic HU measurements for these subjects. Of the 26 scans that met <5th percentile cutoff, 17 (65.4%) were identified as FP by radiologist review. In contrast, only 6 (26%) scans in the 5th-10th percentile cutoff were identified as FP.

Next, we analyzed the univariate associations between BMI, pancreatic volume, body metrics, diabetes status, and HbA_1c with mean pancreatic HU. Using the 5th percentile of mean pancreatic HU, the odds ratios were significant for incremental increase in BMI (OR 1.07), visceral fat volume (OR 1.37), total fat volume (OR 1.12), and presence of diabetes mellitus type 1 but not type 2 (OR 6.76). When using the 10th percentile instead, this also included subcutaneous fat volume (OR 1.26) and muscle volume (OR 1.69) (Table 2).

A total of 46 pre-diagnostic CT examinations from PDAC cases (i.e. CT examinations of patients performed 2 months to 2 years prior to radiographic diagnosis of PDAC) were compared to 92 age, sex, and diabetes mellitus matched controls [Supplementary Table 5]. BMI and mean pancreatic HU were both significantly lower in cases compared to controls (Fig. 3). Using logistic regression analysis, the odds for developing PDAC was significantly higher with decreasing BMI and decreasing mean pancreatic HU in a

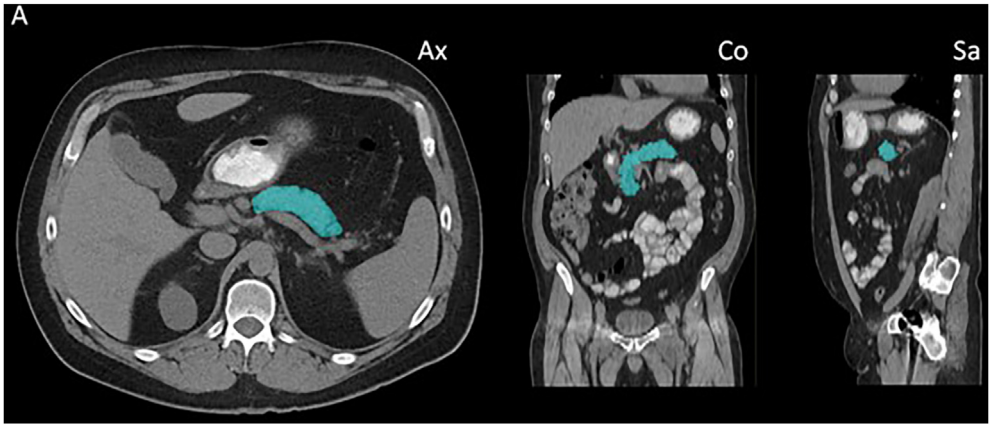

Fig. 1. Example of CNN-based pancreas segmentation in RIL-Contour. Segmentation is done on the axial slices (Ax) and reconstructed in real time of the coronal (Co) and sagittal (Sa) views. CNN, convolutional neural network; RIL, radiology informatics laboratory.

Table 1
Examination Parameters and Demographics per sex category.

	Total (N = 469)	Female (N = 236)	Male (N = 233)	P-value
BMI				
Mean (SD)	30.2 (7.9)	30.7 (8.7)	29.6 (6,9)	0.1242[a]
Median	28.8	28.8	28.9	
Age				
Mean (SD)	52.1 (18.6)	50.7 (18.7)	52.5 (18.6)	0.2891[a]
Median	50.4	49	54	
Diabetes Mellitus				
No	362 (77.2%)	186 (78.8%)	176 (75.5%)	
Yes	107 (22.8%)	50 (21.2%)	57 (24.5%)	0.4415[b]
DM type 1	12 (11.2%)	8 (16%)	4 (7%)	
DM type 2	95 (88.8%)	42 (84%)	53 (93%)	0.2191[b]
Pancreas Volume (cm^3)				
Mean (SD)	86.07 (32.25)	74.76 (25.58)	97.53 (34.25)	<0.0001[c]
Mean Pancreatic HU				
Mean (SD)	15.4 (21.1)	19.4 (19.5)	11.4 (21.8)	<0.0001[c]

Table 1. Demographic characteristics (BMI, age, and diabetes mellitus) and pancreas examination parameters (pancreas volume and mean pancreatic HU) of study participants per sex category. Continuous variables are reported as means (with SD) and discrete variables are reported as total numbers (with percentages). For BMI, 2 female and 8 male values are missing. SD, standard deviation; DM, Diabetes Mellitus; HU, Hounsfield Unit.

[a] One-way ANOVA (unpaired *t*-test).
[b] Fisher's exact test.
[c] Kruskal Wallis test.

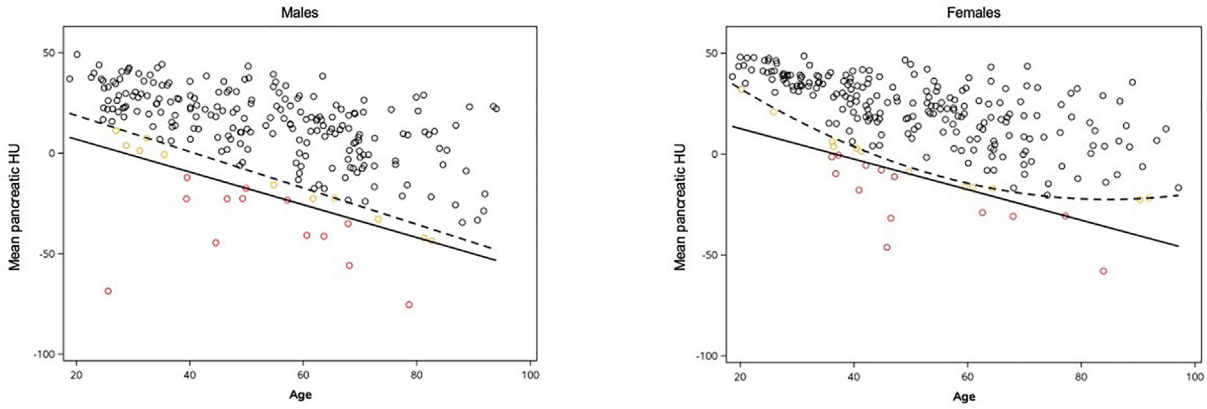

Fig. 2. Visual representation of the distribution of mean pancreatic HU in males (left) and females (right). The dotted lines represent the cutoff at the lowest 10% and the solid lines represent the cutoff at the lowest 5% of pancreatic HU based on quantile regression. Female 10th percentile uses quadratic function of age; all others use linear function. HU, Hounsfield Unit.

Table 2
Univariate associations between different factors and increased intrapancreatic fat based on 5th and 10th percentile cut-offs.

5th percentile cutoff	Odds ratio (95% CI)	p-value	*10th percentile cutoff*	Odds ratio (95% CI)	p-value
BMI (per 1-point increase)	1.07 (1.03, 1.11)	**0.0009**	**BMI (per 1 point-increase)**	1.07 (1.04, 1.11)	**<.0001**
Pancreas volume (cm^3)	1.00 (0.99, 1.02)	0.6499	**Pancreas volume (cm^3)**	1.01 (1.00,1.02)	0.0959
Subcutaneous fat volume (cm^3)	1.09 (0.96, 1.24)	0.1884	**Subcutaneous fat volume (cm^3)**	1.26 (1.14,1.39)	**<.0001**
Visceral fat volume (cm^3)	1.37 (1.15, 1.64)	**0.0004**	**Visceral fat volume (cm^3)**	1.44 (1.25,1.66)	**<.0001**
Total fat volume (cm^3)	1.12 (1.03, 1.22)	**0.0062**	**Total fat volume (cm^3)**	1.21 (1.13,1.30)	**<.0001**
Muscle volume (cm^3)	1.15 (0.69, 1.92)	0.5955	**Muscle volume (cm^3)**	1.69 (1.16,2.48)	**0.0068**
Diabetes Mellitus	1.86 (0.81–4.31)	0.1456	**Diabetes Mellitus**	2.16 (1.15,4.04)	**0.0160**
DM type I	6.76 (1.68, 27.28)	**0.0072**	DM type I	5.34 (1.52,18.74)	**0.0089**
DM type II	1.37 (0.52, 3.57)	0.5220	DM type II	1.85 (0.94,3.63)	0.0758
HbA1c (per 1 unit increase)	1.25 (0.86, 1.82)	0.2400	**HbA1c (per 1 unit increase)**	1.25 (0.93,1.67)	0.1338

Table 2. Univariate associations between demographic (BMI, diabetes, HbA1c) and metric (pancreas volume, subcutaneous fat volume, visceral fat volume, total fat volume, and muscle volume; all per 1 unit increase) parameters and increased pancreatic fat based on the 5th and 10th percentile mean pancreatic HU cut-offs. CI, confidence interval; BMI, body mass index; DM, Diabetes Mellitus; HbA1c, hemoglobin A1c; HU, Hounsfield Unit.

multivariate model (Table 3).

4. Discussion

In this study, using 19,456 images from 469 patients without known pancreatic disease and aided by whole gland pancreas

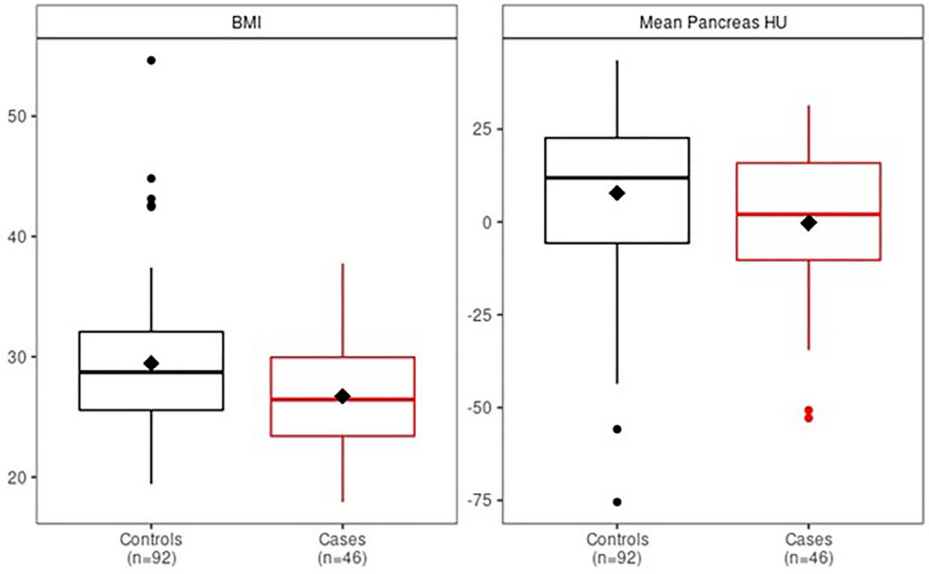

Fig. 3. Boxplot demonstrating the difference in BMI and mean pancreatic HU between controls (n = 92) and PDAC cases (n = 46). Mean BMI (kg/m^2) was significantly lower in PDAC cases versus controls (26.7 vs 29.5; $p = 0.006$). Mean pancreas HU was also significantly lower in PDAC cases versus controls (−0.2 vs 7.8; $p = 0.026$). BMI, Body Mass Index; HU, Hounsfield Unit; PDAC, Pancreatic Ductal Adenocarcinoma.

Table 3
Multivariate logistic regression analysis for the odds of developing PDAC.

	Odds ratio (95% CI)	p-value
BMI (per 1 point decrease)	1.144 (1.041−1.256)	**0.0049**
Mean pancreas HU (per 1 unit decrease)	1.024 (1.003−1.045)	**0.0238**

Table 3. Multivariate odds ratios for developing PDAC with decrease in BMI and mean pancreatic HU. PDAC, Pancreatic Ductal Adenocarcinoma; HU, Hounsfield Unit.

segmentation CNN, we have established the lower 5th and 10th percentile of mean whole gland pancreatic HU on non-contrast abdominal CT examinations across a spectrum of age and sex. Additionally, using this approach in pre-diagnostic non-contrast CT scans in patients with PDAC, we demonstrate a significantly lower mean pancreatic HU in cases compared to age and sex matched controls.

It is well known that a lower mean pancreatic HU reflects increased fat content of the pancreas, and this is based on the principle that adipose tissue and pancreatic parenchymal tissue have distinctively different normal HU ranges (−150 to −30 vs + 30 to +50, respectively) [22].

It has been previously reported that intrapancreatic fat volume increases with age [28]. The primary objective of our study was to establish 'normal' HU values across a spectrum of age and sex in a cohort of subjects without underlying pancreatic disease and for the first time include the whole gland instead of regions of interest to avoid sampling bias. In alignment with prior observations, in this study we noted that mean pancreatic HU decreases as age increases. In our cohort, we also noted that men had lower mean pancreatic HU and higher mean pancreatic volume compared to women. Similar to the study by Saisho et al. that demonstrated a linear relationship between intrapancreatic fat and BMI, we established a linear relationship between mean pancreatic HU and BMI [28]. When comparing mean pancreatic HU between patients with and without diabetes mellitus, the mean whole pancreatic HU in diabetes mellitus patients was significantly lower. This finding is also consistent with previous studies that have shown an association between diabetes mellitus and intrapancreatic fat measured by either ultrasound echogenicity [29] or MRS [20]. Saisho et al. did not demonstrate a difference in pancreatic fat volume in patients with diabetes mellitus compared to those without [28]. However, they used volumetric data rather than mean attenuation for pancreatic fat estimation. To calculate pancreatic fat volume, they subtracted pancreatic parenchymal volume (as defined by tissue that was visible at a +40 HU window) from total pancreatic volume, a limitation that we were able to overcome in our study by using whole gland segmentation and mean HU estimation. In addition, the use of CT examinations with IV contrast (rather than non-contrast CT) in previous assessments of FP would alter the normal HU range of parenchymal tissue used to define pancreas parenchyma (i.e. +30 to +50).

Our study is the first to calculate whole pancreas mean attenuation on non-contrast CT using whole gland analysis and correlate the results with body composition. Matsumoto et al. described different subtypes of fatty replacement, noting that fat is often distributed unevenly in the pancreas [11]. This finding highlights the inherent limitation of non-invasive methods of pancreatic fat assessment that use ROIs (regions of interest) instead of whole gland analysis. To obtain information about the whole pancreas on a CT scan, every slice in all imaging planes needs to be reviewed for presence of pancreatic tissue and manually outlined for an accurate assessment. This is a time-consuming process and unless this process can be automated, measurements obtained by this method will not be clinically translatable. Convolutional neural networks (CNNs), a form of machine learning, have been used to automatically segment organs such as liver, heart, or kidneys with high levels of Dice similarity indices [30]. The pancreas typically scores lower on the Dice similarity index, likely due to the high interperson variability in shape, size, and location of the pancreas in the abdomen. In our study, we started by manually demarcating the pancreas and used this data to train a CNN to segment the pancreas on non-contrast CT. Although for the purposes of this study all the examinations included in our data analysis were either segmented manually or manually corrected after CNN-assisted segmentation, we were able to train a CNN in the process that we intend to validate in future studies. By calculating the normal spectrum of

pancreatic HU across age and sex, we were able to establish the 5th and 10th percentiles of mean pancreatic HU per age and sex category. Using these percentiles as threshold values for abnormal intrapancreatic fat, we noted an association with increase in BMI, visceral fat volume, total fat volume, and diabetes mellitus type 1 (but not type 2). These values could provide a criterion standard to study histologic correlation with intrapancreatic fat and systematically study the implications of increased intrapancreatic fat on pancreatic and metabolic diseases.

The association between PDAC and obesity is well established [5]. Silverman et al. noted that obesity was associated with a 60% excess risk of PDAC and this was independent of age and sex [4]. At least two studies have specifically investigated intrapancreatic fat content in pancreas resection specimens of patients with PDAC or pancreatic intraepithelial neoplasia (PanIN). Rebours et al. demonstrated that the number of PanIN lesions in pancreatic resection specimens was associated with the degree of intrapancreatic fat infiltration, but not BMI [31]. Hori et al. noted an increase in fatty infiltration in pancreas specimens with PDAC compared to pancreas specimens of patients without PDAC [7]. However, both these studies assess the amount of intrapancreatic fat at the time of diagnosis, raising the question whether increased intrapancreatic fat is a risk factor or rather a consequence of pancreatic neoplasia.

In this study, using pre-diagnostic CT examinations, we demonstrate that patients who subsequently developed PDAC had lower mean pancreatic HU (measured at a timepoint before any radiographic evidence of pancreatic neoplasm) compared to age, sex, and diabetes mellitus matched controls who did not develop PDAC. This is an early but significant observation in the field of early detection of pancreatic cancer and possibly identifies a novel risk factor. Interestingly, we also note that the average BMI was lower in the group of pre-diagnostic PDAC patients compared to their matched controls. This finding is likely due to the well-described phenomenon of pathological weight loss that predates a diagnosis of PDAC [32]. We did not find a significant difference in pancreas volume in this pre-diagnostic phase indicating that the significantly lower mean HU in this group is unlikely to be secondary to pancreatic atrophy. Overall, our findings support the hypothesis that a lower mean whole gland pancreatic attenuation is a novel risk factor for PDAC and validation in larger cohorts is warranted.

Our study had several limitations. First, our study population predominantly included Caucasian (97%) subjects and thus we are unable to confirm if these normal ranges and thresholds hold true in other racial groups. However, this novel approach of whole gland segmentation and analysis described in this study can be used to study a more diverse population. Second, since this was a retrospective study using CT images from both inpatient and outpatient visits, our study cohort might not represent a true 'population' cohort. Yet, the use of a large sample set of images and systematically avoiding bias in patient and scan selection strengthens the validity of our results. Third, we acknowledge that subtle pancreatic disease could be missed on examinations that used non-contrast CT only. Nonetheless, every report was read by an experienced abdominal radiologist explicitly noting the absence of pancreatic pathology. Fourth, we were not able to correlate our whole pancreas attenuation thresholds with pancreas histology due to the unavailability of pancreas tissue specimens in individuals without pancreatic disease. Fifth, given the inherent limitations of non-contrast CT, segmentation could not reliably exclude non-calcified blood vessels running through the pancreas parenchyma or the possibility of small amounts of peripancreatic fat at the gland margin being included the segmentations. However, vascular calcifications when present were excluded. We also note that almost 40% of the scans from our cohort without underlying pancreatic diseases had a slice thickness of 5 mm or more. While this could have resulted in failure to identify small focal pancreatic lesions, it is unlikely to have significant impact on estimates of average pancreatic HU or volume. Lastly, although a CNN was optimized and used to facilitate segmentation, all scans underwent thorough rigorous manual review prior to establishing normal values. The CNN for pancreas segmentation on non-contrast CTs needs independent validation for clinical translation.

In summary, in this study we report for the first time, mean pancreas HU values on non-contrast CT in a cohort of adults without underlying pancreatic disease across a spectrum of age and sex. Using whole organ segmentation, we demonstrate association of low mean pancreatic HU with intra-abdominal visceral adiposity and our findings support previously reported associations between increased intrapancreatic fat and increasing age, BMI, and diabetes mellitus. We have also demonstrated that pancreatic mean HU is significantly lower in the pre-diagnostic phase of PDAC compared to cancer-free controls matched for age, sex, and glycemic status, indicating that this may be a radiologic risk factor or an imaging feature that predates the onset of overt PDAC. This early finding will need to be validated in larger independent cohorts.

Declaration of competing interest statement and disclosures

As co-inventor on licensed technologies, S.M. could share potential future royalties to Mayo Clinic from Exact Sciences in accordance with institutional policy and oversight. V.C. provides consulting for Interpace Diagnostics and is a shareholder of Nevakar Corporation. S.V. contributes to UpToDate chapters. The other authors of this manuscript have no conflict of interest to declare.

Appendix A. Supplementary data

Supplementary data to this article can be found online at https://doi.org/10.1016/j.pan.2021.08.004.

Funding sources

This study was supported by Award Number P50 CA102701 (Mayo Clinic SPORE in Pancreatic Cancer). The content is solely the responsibility of the authors and does not necessarily represent the official views of the National Cancer Institute or the National Institutes of Health.

References

[1] Smits MM, Van Geenen EJM. The clinical significance of pancreatic steatosis. Nat Rev Gastroenterol Hepatol 2011;8(3):169–77. https://doi.org/10.1038/nrgastro.2011.4.
[2] Mathur A, Marine M, Lu D, et al. Nonalcoholic fatty pancreas disease. HPB 2007;9(4):312–8. https://doi.org/10.1080/13651820701504157.
[3] Patel S, Bellon EM, Haaga J, Park CH. Fat replacement of the exocrine pancreas. Am J Roentgenol 1980;135(4):843–5. https://doi.org/10.2214/ajr.135.4.843.
[4] Silverman DT, Swanson CA, Gridley G, et al. Dietary and nutritional factors and pancreatic cancer: a case-control study based on direct interviews. J Natl Cancer Inst 1998;90(22):1710–9. https://doi.org/10.1093/jnci/90.22.1710.
[5] Arslan AA, Helzlsouer KJ, Kooperberg C, et al. Anthropometric measures, body mass index, and pancreatic cancer: a pooled analysis from the pancreatic cancer cohort consortium (PanScan). Arch Intern Med 2010;170(9):791–802. https://doi.org/10.1001/archinternmed.2010.63.
[6] Genkinger JM, Kitahara CM, Bernstein L, et al. Central adiposity, obesity during early adulthood, and pancreatic cancer mortality in a pooled analysis of cohort studies. Epidemiol Res Progr 2015;26:2257–66. https://doi.org/10.1093/annonc/mdv355.
[7] Hori M, Takahashi M, Hiraoka N, et al. Association of pancreatic fatty infiltration with pancreatic ductal adenocarcinoma. Clin Transl Gastroenterol 2014;5. https://doi.org/10.1038/ctg.2014.5.
[8] Tomita Y, Azuma K, Nonaka Y, et al. Pancreatic fatty degeneration and fibrosis as predisposing factors for the development of pancreatic ductal

adenocarcinoma. Pancreas 2014;43(7):1032–41. https://doi.org/10.1097/MPA.0000000000000159.
[9] Wang H, Maitra A, Wang H. Obesity, intrapancreatic fatty infiltration, and pancreatic cancer. Clin Canc Res 2015;21(15):3369–71. https://doi.org/10.1158/1078-0432.CCR-15-0718.
[10] Majumder S, Philip NA, Takahashi N, Levy MJ, Singh VP, Chari ST. Fatty pancreas: should we Be concerned? Pancreas 2017;46(10):1251–8. https://doi.org/10.1097/MPA.0000000000000941.
[11] Matsumoto S, Mori H, Miyake H, et al. Uneven fatty replacement of the pancreas: evaluation with CT. Radiology 1995;194(2):453–8. https://doi.org/10.1148/radiology.194.2.7824726.
[12] Marks WM, Filly RA, Callen PW. Ultrasonic evaluation of normal pancreatic echogenicity and its relationship to fat deposition. Radiology 1980;137(2):475–9. https://doi.org/10.1148/radiology.137.2.7433680.
[13] Al-Haddad M, Khashab M, Zyromski N, et al. Risk factors for hyperechogenic pancreas on endoscopic ultrasound: a case-control study. Pancreas 2009;38(6):672–5. https://doi.org/10.1097/MPA.0b013e3181a9d5af.
[14] Lee JS, Kim SH, Jun DW, et al. Clinical implications of fatty pancreas: correlations between fatty pancreas and metabolic syndrome. World J Gastroenterol 2009;15(15):1869–75. https://doi.org/10.3748/wjg.15.1869.
[15] Gaborit B, Abdesselam I, Kober F, et al. Ectopic fat storage in the pancreas using 1 H-MRS: importance of diabetic status and modulation with bariatric surgery-induced weight loss. Int J Obes 2015;39(3):480–7. https://doi.org/10.1038/ijo.2014.126.
[16] Heni M, Machann J, Staiger H, et al. Pancreatic fat is negatively associated with insulin secretion in individuals with impaired fasting glucose and/or impaired glucose tolerance: a nuclear magnetic resonance study. Diabetes Metab Res Rev 2010;26(3):200–5. https://doi.org/10.1002/dmrr.1073.
[17] Tushuizen ME, Bunck MC, Pouwels PJ, et al. Pancreatic fat content and β-cell function in men with and without type 2 diabetes. Diabetes Care 2007;30(11):2916–21. https://doi.org/10.2337/dc07-0326.
[18] Hu HH, Kim HW, Nayak KS, Goran MI. Comparison of fat-water MRI and single-voxel MRS in the assessment of hepatic and pancreatic fat fractions in humans. Obesity 2010;18(4):841–7. https://doi.org/10.1038/oby.2009.352.
[19] Hannukainen JC, Borra R, Linderborg K, et al. Liver and pancreatic fat content and metabolism in healthy monozygotic twins with discordant physical activity. J Hepatol 2011;54(3):545–52. https://doi.org/10.1016/j.jhep.2010.07.029.
[20] Lingvay I, Esser V, Legendre JL, et al. Noninvasive quantification of pancreatic fat in humans. J Clin Endocrinol Metab 2009;94(10):4070–6. https://doi.org/10.1210/jc.2009-0584.
[21] Kato S, Iwasaki A, Kurita Y, et al. Three-dimensional analysis of pancreatic fat by fat-water magnetic resonance imaging provides detailed characterization of pancreatic steatosis with improved reproducibility. PLoS One 2019;14(12):e0224921. https://doi.org/10.1371/JOURNAL.PONE.0224921.
[22] Wegener OH, Fassel R, Welger D, Wegener OH. Whole-body computed tomography. Blackwell Scientific Publications; 1993.
[23] Schmitz-Moormann P, Pittner PM, Heinze W. Lipomatosis of the pancreas: a morphometrical investigation. Pathol Res Pract 1981;173(1–2):45–53. https://doi.org/10.1016/S0344-0338(81)80006-4.
[24] Philbrick KA, Weston AD, Akkus Z, et al. RIL-contour: a medical imaging dataset annotation tool for and with deep learning. J Digit Imag 2019;32(4):571–81. https://doi.org/10.1007/s10278-019-00232-0.
[25] Ronneberger O, Fischer P, Brox T. U-net: convolutional networks for biomedical image segmentation. In: Lecture notes in computer science (including subseries lecture notes in artificial intelligence and lecture notes in bioinformatics), vol. 9351. Springer Verlag; 2015. p. 234–41. https://doi.org/10.1007/978-3-319-24574-4_28.
[26] Weston AD, Korfiatis P, Kline TL, et al. Automated abdominal segmentation of CT scans for body composition analysis using deep learning. Radiology 2019;290(3):669–79. https://doi.org/10.1148/radiol.2018181432.
[27] Koenker R, Hallock KF. Quantile regression. J Econ Perspect 2001;15(4):143–56. https://doi.org/10.1257/jep.15.4.143.
[28] Saisho Y, Butler AE, Meier JJ, et al. Pancreas volumes in humans from birth to age one hundred taking into account sex, obesity, and presence of type-2 diabetes. Clin Anat 2007;20(8):933–42. https://doi.org/10.1002/ca.20543.
[29] Wang CY, Ou HY, Chen MF, Chang TC, Chang CJ. Enigmatic ectopic fat: prevalence of nonalcoholic fatty pancreas disease and its associated factors in a Chinese population. J Am Heart Assoc 2014;3(1). https://doi.org/10.1161/JAHA.113.000297.
[30] Chu C, Oda M, Kitasaka T, et al. Multi-organ segmentation based on spatially-divided probabilistic atlas from 3D abdominal CT images. In: Lecture notes in computer science (including subseries lecture notes in artificial intelligence and lecture notes in bioinformatics), vol. 8150. Berlin, Heidelberg: LNCS. Springer; 2013. p. 165–72. https://doi.org/10.1007/978-3-642-40763-5_21.
[31] Rebours V, Gaujoux S, D'Assignies G, et al. Obesity and fatty pancreatic infiltration are risk factors for pancreatic precancerous lesions (PanIN). Clin Canc Res 2015;21(15):3522–8. https://doi.org/10.1158/1078-0432.CCR-14-2385.
[32] Sah RP, Sharma A, Nagpal S, et al. Phases of metabolic and soft tissue changes in months preceding a diagnosis of pancreatic ductal adenocarcinoma. Gastroenterology 2019;156(6):1742–52. https://doi.org/10.1053/j.gastro.2019.01.039.